Mesoscale Gravity Waves in Moist Baroclinic Jet-Front Systems

Junhong Wei and Fuqing Zhang, Pennsylvania State University

Contact: jwei@psu.edu
fzhang@psu.edu

Introduction and Model Description

Complementary to Zhang (2004) on the generation of mesoscale waves in dry baroclinic jet-front systems, a series of convection-permitting simulations with the Weather Research and Forecast (WRF) model are performed to study mesoscale gravity waves in the moist baroclinic waves with varying degree of convective instability. These idealized experiments are initialized with the same baroclinic jet but with different initial moist content. To be specific, EXP00-EXP80 have 00%-80% initial relative humidity of that in EXP100.

Overview on Simulated Baroclinic Waves and Gravity Waves

Same Initial Baroclinic Jet + Higher initial Moisture Content

- **Faster growth of baroclinic wave in terms of eddy kinetic energy (EKE-BW)**
- **Faster growth of eddy kinetic energy for gravity waves (EKE-GW)**
- **Greater EKE-GW when EKE-BW at similar amplitude of ~52.5 m^2s^{-2}**

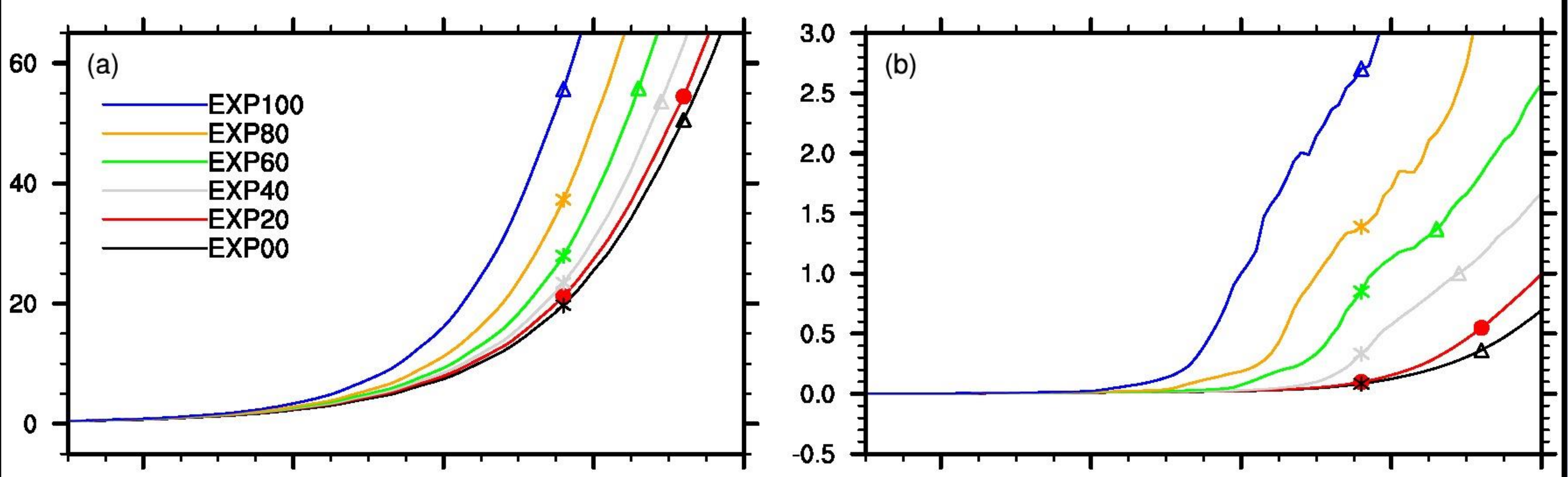

Figure 1. Time series (h) of eddy kinetic energy (m^2s^{-2}) for (a) EKE-BW (baroclinic wave component), (b) EKE-GW (gravity wave component) during 50-140 h.

EXP00	Dry Localized Identifiable Gravity Wave Modes Generated By Dry Source
EXP20	Dry Gravity Wave Modes Continue to Dominate; Similar Wave Characteristics With those in EXP00; The Amplitude of WP5 Is Enhanced By ~2 Times; Modification in WP3.
EXP40	Both Shorter-Scale Waves and Intermediate-Scale Waves Are Essential.
EXP60	More Variances of Shorter-Scale Gravity Waves In the Jet Exit Region.
EXP80	Shorter-Scale Wave Signatures Filling the Jet; Imprint of Intermediate-Scale Wave Signatures South of the Upper-Level Northwesterly Jet
EXP100	Particularly Hard to Determine the Dominant Orientation of Wave Front South of the Upper-Level Northwesterly Jet

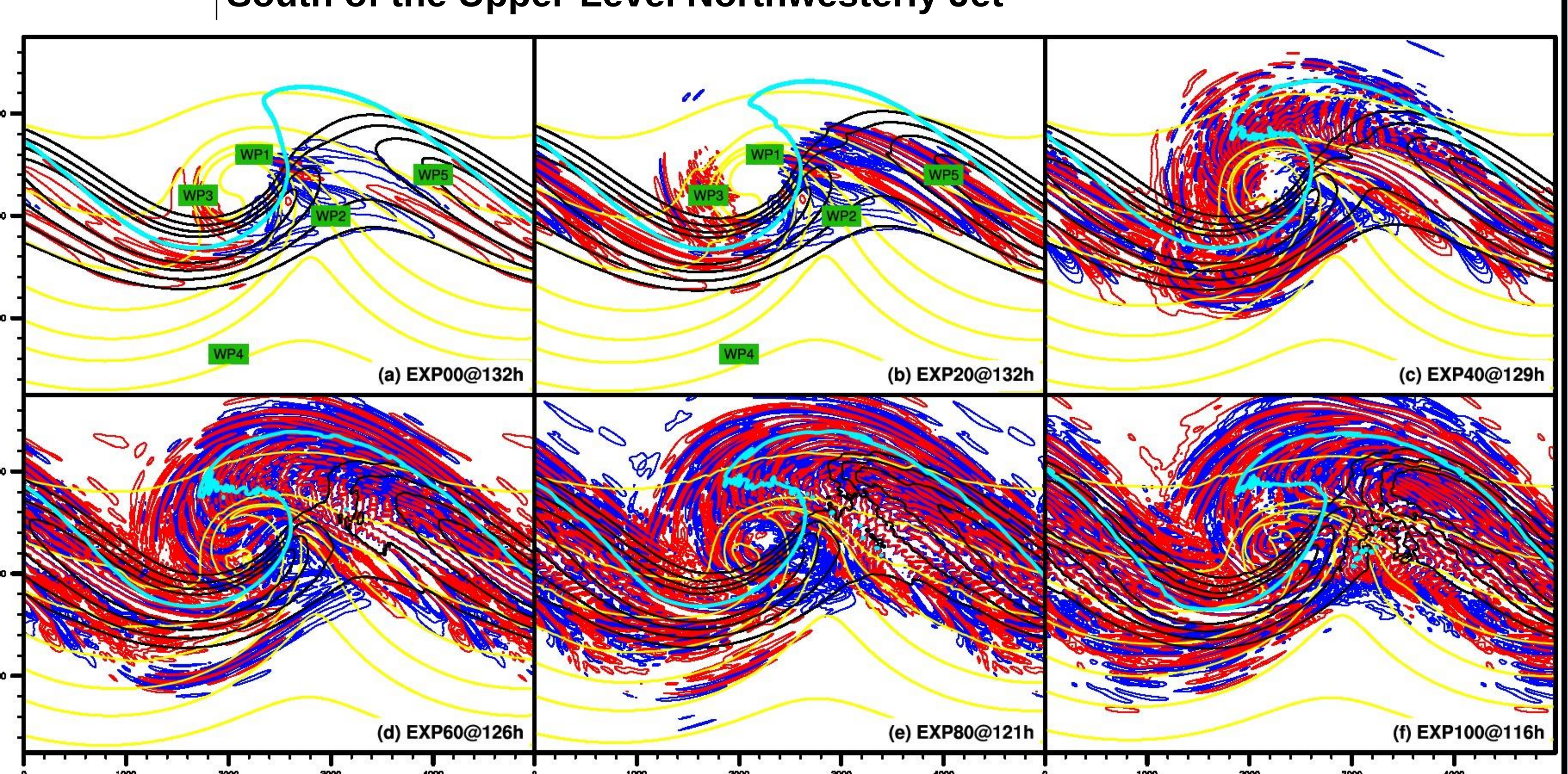

Figure 2. Simulated 1-km temperature (yellow lines), 8-km horizontal wind (black lines), 12-km horizontal divergence (blue/red lines, positive/negative), and 7-km dynamic tropopause (turquoise lines).

Wave Identification

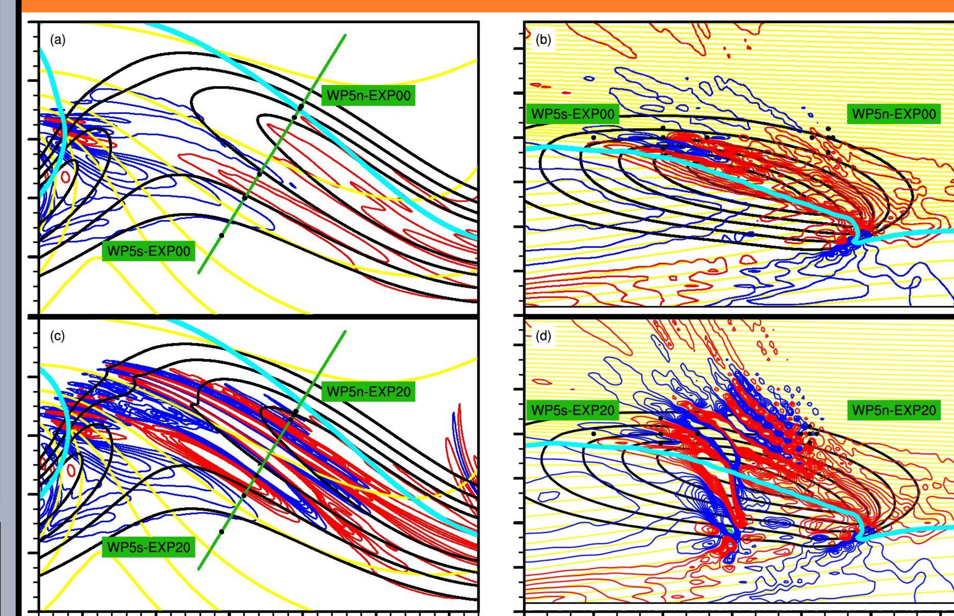

Figure 3. Comparison of WP5 at 132 h between EXP00 (a,b) and EXP20 (c,d) in horizontal (a,c) and vertical (b,d) view.

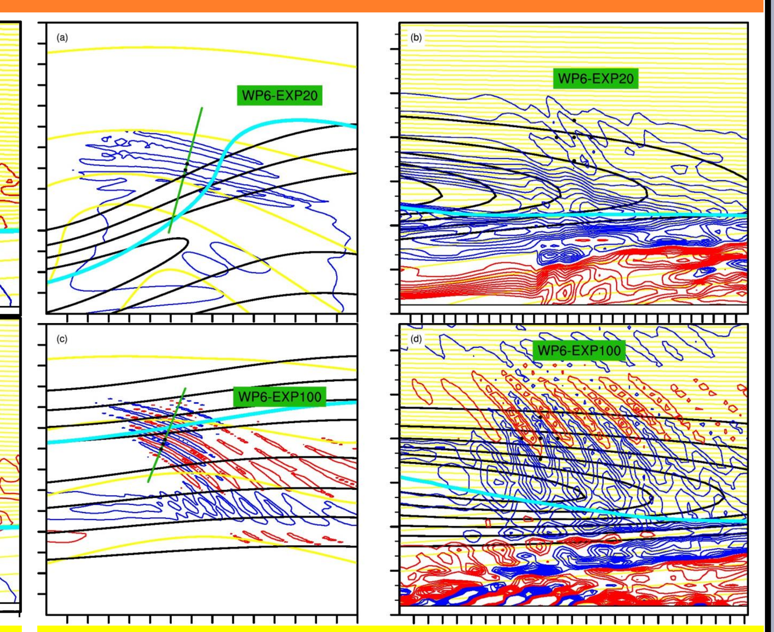

Figure 4. Same as Figure 3, but for WP6 between EXP20 (a,b) at 110 h and EXP100 (c,d) at 72 h.

WP-EXP	Λh (km)	Λz (km)	Ω (10-4 s-1)
WP5s-EXP00	490	1.4	1.2
WP5n-EXP00	90	1.6	3.9
WP5s-EXP20	450	1.7	1.3
WP5n-EXP20	68	1.1	3.6
WP6-EXP20	62	2.8	9.2
WP6-EXP100	50	2.9	12.0

- **WP1, WP2 and WP4 are close between EXP00 and EXP20.**
- **For WP3 upstream of convection, another similarly bended WP3b-EXP20 is found to the west of the cyclone center. For WP5 downstream of the convection, the wave characteristics are generally similar between EXP00 and EXP20 (Fig. 3; Table 1). However, The amplitude of WP5 in EXP20 is much stronger.**
- **A potentially new mode of gravity waves WP6 (Fig. 4) is identified before WP1-WP5 become mature.**

Table 1 (Above): Summary of the gravity wave characteristics. Column 1-4 represent the wave packets, the simulated horizontal wavelengths, vertical wavelengths, and the intrinsic frequencies derived from dispersion relationship.

Evolution of WP5 and Its Sensitivity to Diabatic Heating

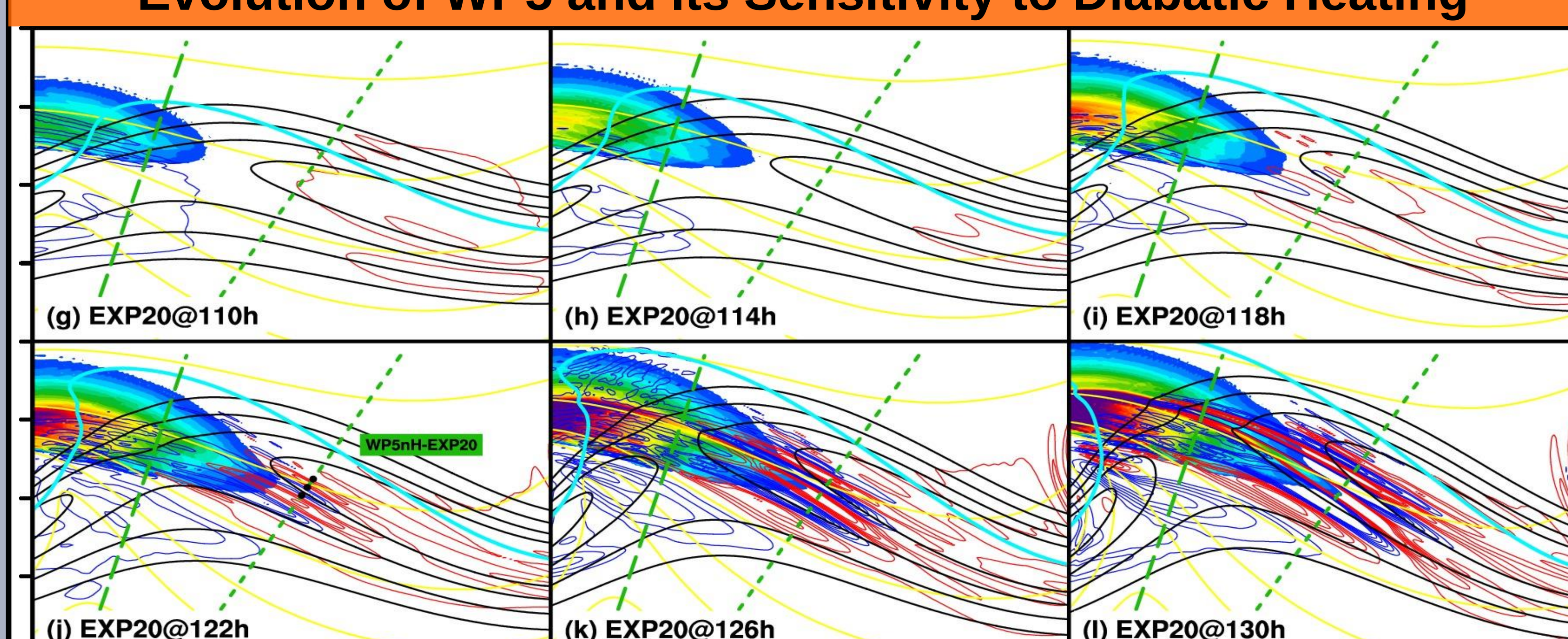

Figure 5. The horizontal evolution of WP5 at every 6 hours from 102 h to 130 h in (g-l) EXP20. Contours follow Fig. 2. The shaded color denotes the vertically averaged positive-only latent heating rate. The distance between tick marks is 500 km.

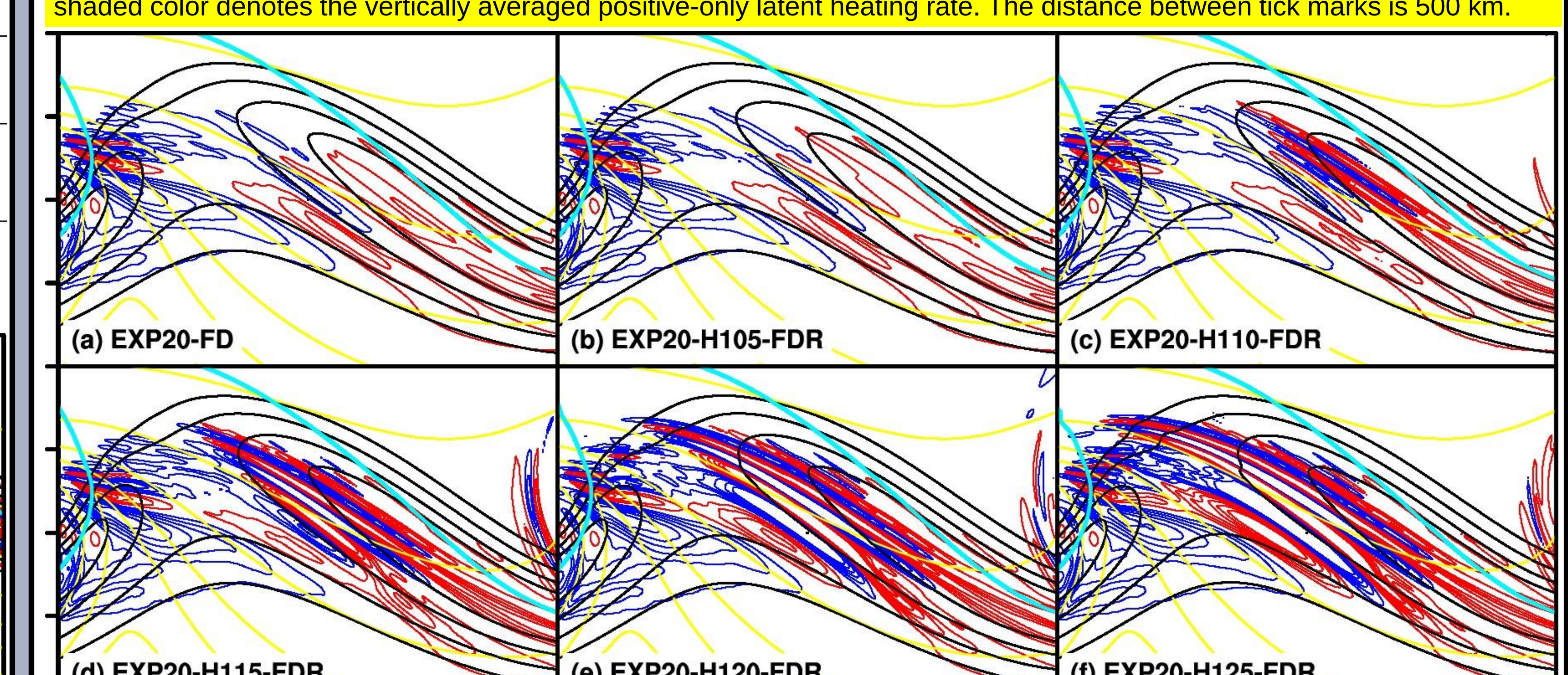

Figure 6. The horizontal view of WP5 at 132 h. Contours follow Fig. 2. EXP20-FD is a complete fake dry run from hour 0. Other fake dry (FDR) experiments consist of full moist runs for 105-130 hours and their FDR restart runs.

- **Differences in gravity waves may travel from upstream localized convection toward downstream jet entrance region. Localized latent heating upstream may have an important impact on the wave disturbance not only locally, but also remotely where there is no heating (Fig. 5).**
- **The more latent heating allowed before turning off, the more similarity between WP5 in the fake dry runs and that in EXP20. Short-duration convection may impact wave signals for a very long period (Fig. 6).**

Tracing Gravity Wave in Moist Baroclinic Waves

- **Generally consistent with Lin and Zhang (2008) for WP1-WP3.**
- **Generally similar tracking for WP1-WP5 between EXP00 and EXP20 (not shown).**
- **The propagation of gravity wave may be sensitive to transient background flow (Fig. 7). For WP5s based on 3D data at 132 h, waves can be traced back to the southwest part of the cyclone, but it take ~7 hours to travel the top 1 km. For WP5s based on 4D WRF data, waves can only travel ~2 hours within ~12 km.**
- **Convection/latent Heating may be the most likely source mechanism for WP6 in EXP20 and EXP100 (not shown).**

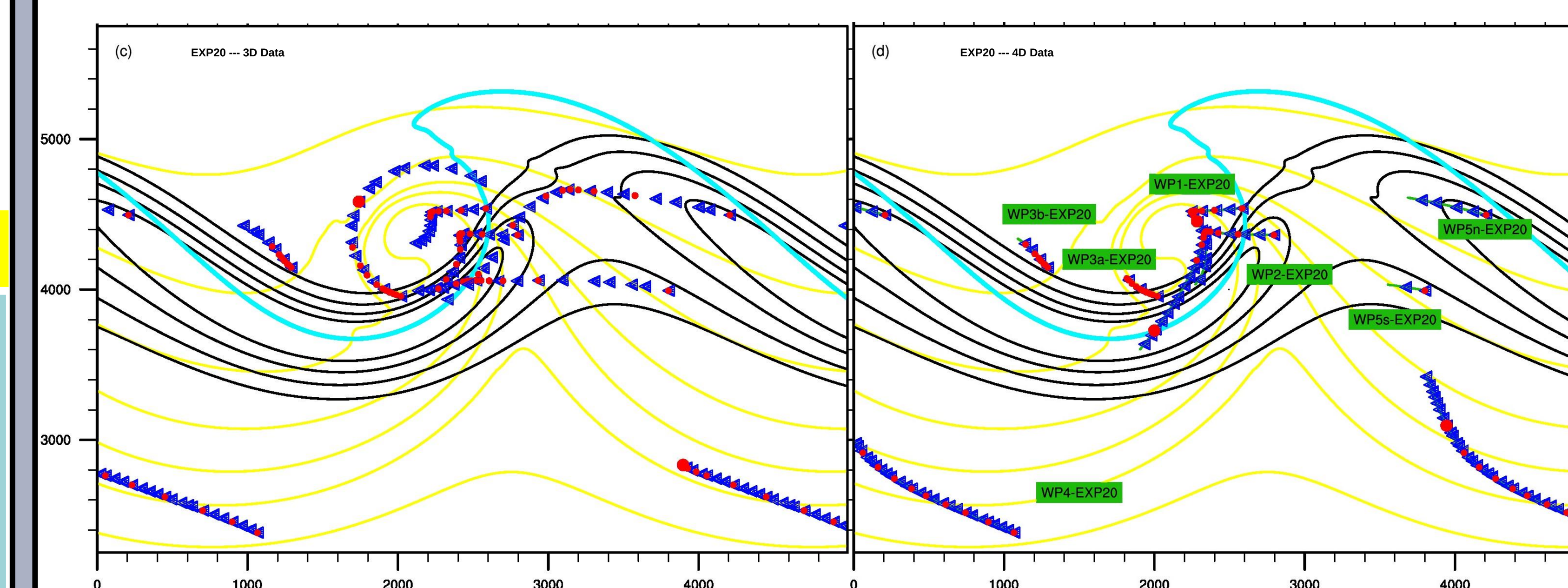

Figure 7. Tracking gravity waves in EXP20 based on GROGRAT, (c) using WRF data at 132 h only, and (d) using WRF data at each hour. Blue triangles (red solid circles) represent traces at each hour (height level).

Discussion and Hypothesis on Gravity Wave Variations

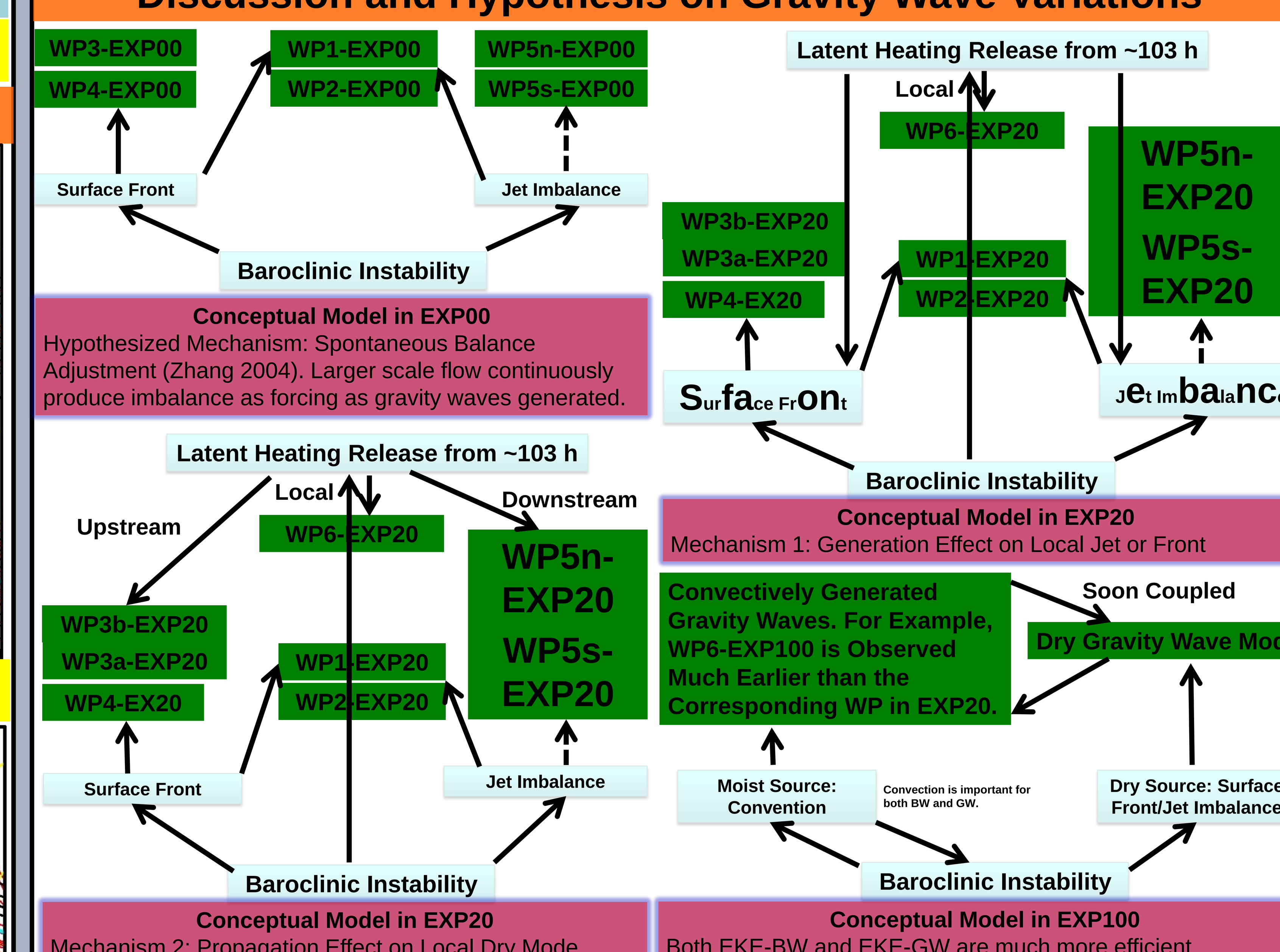

Concluding Remarks

The dry experiment reproduces the gravity wave modes simulated in Zhang (2004). Under weak convective instability with small amount of moisture, dry dynamic gravity wave modes continue to dominate. However, convective gravity wave mode is observed before dry gravity wave modes become mature. For gravity wave downstream of the convection, wave amplitudes are noticeably enhanced. Under strong convective instability with full moisture content, convection-generated gravity waves are observed much earlier than that with reduced moisture content. The convective mode is soon fully coupled with other gravity wave modes and background flow as baroclinicity increases over time.

Reference

Zhang, F., 2004: Generation of mesoscale gravity waves in the upper-tropospheric jet-front systems. *J. Atmos. Sci.*, 61, 440-457.

Lin, Y., and F. Zhang, 2008: Tracking gravity waves in baroclinic jet-front systems. *J. Atmos. Sci.*, 65, 2402-2415.

Acknowledgments: We are very grateful to Chris Davis for providing the codes for PV inversion, to Steve Eckmann for GROGRAT, and to Shuguang Wang for his help on setting up the idealized simulation. Informal reviews by Yongqiang Sun were thorough and helpful. This research is supported by the National Science Foundation.